Yeast Protein Farnesyltransferase: Steady-State Kinetic Studies of Substrate Binding†

Julia M. Dolence,‡ Pamela B. Cassidy, Jeffery R. Mathis,§ and C. Dale Poulter*

Department of Chemistry, University of Utah, Salt Lake City, Utah 84112

Received August 16, 1995; Revised Manuscript Received October 11, 1995⊗

ABSTRACT: Protein farnesyltransferase (PFTase) catalyzes the alkylation of cysteine in C-terminal CaaX sequences of a variety of proteins, including Ras, nuclear lamins, large G-proteins, and phosphodiesterases, by farnesyl diphosphate (FPP). These modifications enhance the ability of the proteins to associate with membranes and are essential for their respective functions. The binding mechanism for yeast PFTase was deduced from a combination of steady-state kinetic and equilibrium studies. Rates for prenylation were measured by a continuous assay based on an enhancement in the fluorescence of the dansyl moiety in pentapeptide dansyl-GCVIA upon farnesylation by FPP. Unreactive substrate analogs for FPP and dansyl-GCVIA gave steady-state inhibition patterns for the dead-end inhibitors typical of an ordered sequential mechanism in which FPP adds to the enzyme before the peptide. The kinetic analysis was complicated by substrate inhibition for dansyl-GCVIA. The substrate inhibition was reversed at high concentrations of FPP, indicating that formation of the nonproductive enzyme−peptide complex is competitive with respect to FPP. Progress curves were fitted to an integrated form of the rate expression to determine the catalytic constant, $k_{cat} = 4.5 \pm 1.9\ s^{-1}$, and the Michaelis constant for dansyl-GCVIA, $K_M^D = 0.9 \pm 0.1\ \mu M$. The dissociation constant for FPP, $K_D = 75 \pm 15$ nM, was measured using a membrane retention assay.

A large family of proteins in eukaryotic organisms has been identified that are posttranslationally modified by the attachment of prenyl groups to C-terminal cysteines through thioether bonds. Members of the family include "true" Ras proteins, other members of the Ras superfamily (Rab, Ral, Rac, Rap), nuclear lamins, large G-proteins, and phosphodiesterases (Clarke, 1992). Ras proteins are major components in the signal transduction pathway leading to cell division, and approximately 30% of human cancers are attributed to mutations in Ras. Both normal and mutant forms of Ras must associate with the inner surface of the outer membrane in order to participate in signal transduction. The discovery that farnesylation is required for oncogenic forms of Ras to manifest their transforming activity has promoted widespread interest in protein prenylation (Clarke, 1992; Schafer et al., 1989; Kohl et al., 1993; James et al., 1993).

Protein farnesyltransferase (PFTase)[1] and protein geranylgeranyltransferase I (PGGTase I) prenylate proteins containing C-terminal CaaX consensus sequences, in which "a" is an aliphatic amino acid and "X" is one of several amino acids, as illustrated in Scheme 1. Both enzymes are heterodimers that share a common α subunit in combination with distinct β subunits (Armstrong et al., 1993). The β subunits, although different, have significant sequence similarity (Zhang et al., 1994). Whether the protein substrate is modified by a farnesyl or a geranylgeranyl group is determined by the X residue. If X is Ser, Ala, Met, Cys, or Gln, then the protein is farnesylated; if X is Leu or Phe, then the protein is geranylgeranylated (Moores et al., 1991; Reiss et al., 1991; Omer et al., 1993; Yokoyama et al., 1991). Two other prenylation recognition motifs have been identified. In the Rab GTP-binding proteins, both cysteines of C-terminal -CC or -CXC sequences are geranylgeranylated by PGGTase II (Farnsworth et al., 1991).

Scheme 1. Reaction Catalyzed by Protein Farnesyltransferase

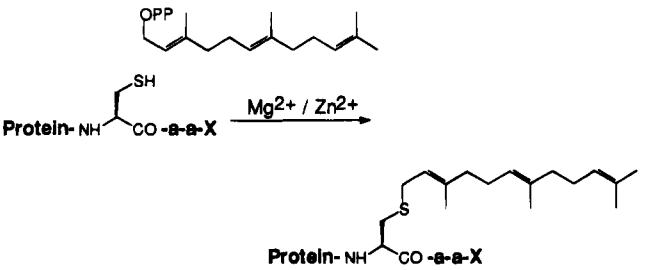

In recent years, there has been an intense search for PFTase inhibitors as potential antitumor agents. Short peptides conforming to the CaaX rule are inhibitors of PFTase, acting either as alternate substrates or as true dead-end inhibitors (usually when a_2 is F, Y, or W) that are competitive for the normal peptide substrate (Brown et al., 1992). Peptidomimetic structures containing cysteine and methionine residues separated by aromatic spacers (Vogt et al., 1995), benzodiazepine spacers (James et al., 1993; Marsters et al., 1994), or by other tethers (Wai et al., 1994) are potent inhibitors *in vitro* and disrupt the growth of Ras-transformed cells. Other inhibitors, such as α-(hydroxyfarnesyl)phosphonic acid

* To whom correspondence should be addressed.

† This work was supported by the National Institutes of Health Grant GM 21328.

‡ NIH Postdoctoral Fellow, GM15286.

§ NIH Postdoctoral Fellow, GM17697.

⊗ Abstract published in *Advance ACS Abstracts,* November 15, 1995.

[1] Abbreviations: AMBA, 3-aminomethylbenzoic acid; AC^{F}VLS, *S*-farnesyl ACVLS; C^{F}VIA, *S*-farnesyl CVIA; KTSC^{F}VFM, *S*-farnesyl KTSCVFM; EDTA, ethylenediaminetetraacetic acid; FPP, farnesyl diphosphate; D, dansyl-GCVIA; DMAPP, dimethylallyl diphosphate; DTT, dithiothreitol; IPP, isopentenyl diphosphate; PFTase, protein farnesyltransferase; PGGTase, protein geranylgeranyltransferase; Tris, tris(hydroxymethyl)aminomethane.

0006-2960/95/0434-16687$09.00/0

(Gibbs et al., 1993), are based on nonhydrolyzable FPP analogs. Still other PFTase inhibitors, such as chaetomellic acid A and zaragozic acid A, have been identified through microbial screens and do not closely resemble either substrate (Tamanoi, 1993).

Steady-state kinetic studies with bovine PFTase and a series of dead-end substrate and product inhibitors indicated a random mechanism for substrate binding (Pompliano et al., 1992a). In further studies with human PFTase, including steady-state kinetic and isotope trapping, Pompliano et al. (1993) concluded that binding was random, but there was a preference for addition of FPP first during formation of a catalytically active ternary enzyme. Furfine et al. (1995) confirmed a functionally ordered binding mechanism for PFTase with pre-steady-state and steady-state studies. These experiments indicated that FPP bound to the enzyme in a two-step process, and the peptide bound to this complex irreversibly. During initial characterization of yeast PFTase, Gomez et al. (1993) established that the substrates bound to PFTase sequentially but did not establish the binding order. In this paper we describe experiments that firmly establish an ordered sequential binding mechanism for yeast PFTase and report potent substrate inhibition with the pentapeptide dansyl-GCVIA.

MATERIALS AND METHODS

Materials. Recombinant yeast PFTase was expressed in *Escherichia coli* (JM101/pGP114) and was purified by ion-exchange and immunoaffinity chromatography as previously described (Mayer et al., 1993). Protein concentrations were measured by the method of Bradford (1976). Dansyl-GCVIA and other CaaX-peptides were synthesized by solid-phase peptide methods. FPP was synthesized by the method of Davisson et al. (1986). *S*-Farnesylcysteine, *S*-farnesyl-cysteine methyl ester, C^FVIA, $KTSC^FVFM$, and AC^FVLS were synthesized by the method of Brown et al. (1991). Ac-C^FVIA was synthesized according to the procedure of Pompliano et al. (1992b). [^{3}H]FPP (15 Ci/mmol) was purchased from DuPont-NEN (Boston, MA) and ARC (St. Louis, MO). *n*-Dodecyl-β-D-maltoside was purchased from CalBiochem. All other chemicals were from Sigma (St. Louis, MO) or Aldrich (Milwaukee, WI) and used without further purification.

Methods. Prenyltransferase Assays. Catalytic rate constants (k_{cat}) were measured using a fluorescence assay that continuously monitored farnesylation of dansylated pentapeptide dansyl-GCVIA (D) (Pompliano et al., 1992b; Cassidy et al., 1995) using a Spex FluoroMax model spectrofluorimeter with λ_{ex} = 340 (slit width = 5.1 or 8.5 nm) and λ_{em} = 486 nm (slit width = 5.1 or 8.5 nm) and 3 mm square cuvettes. Assays (250 μL) were conducted at 30 °C in 50 mM Tris HCl, 10 mM $MgCl_2$, 10 μM $ZnCl_2$, 5 mM DTT, 0.04% (w/v) *n*-dodecyl-β-D-maltoside, pH 7.0. Nonsaturating substrate concentrations (for K_i and IC_{50} determinations) were 0.9 or 2.4 μM for dansyl-GCVIA and 2 μM for FPP. PFTase (0.5−4.0 nM) was used to initiate the reactions. The saturating FPP concentration used for V_{Max} and K_M^D determinations was 100−300 μM. For continuous assays, measurements were obtained every 10 s for at least 15 min. For initial velocity studies, rates were measured from the linear region of each run, and all measurements were made in duplicate. Rates were measured in counts per second per second and converted to units of μM s^{-1} using a conversion factor (m) calculated from the slope of a line generated in a plot of concentration of synthetic dansyl-G(*S*-farnesyl)CVIA (dansyl-GC^FVIA) versus fluorescence intensity (Cassidy et al., 1995).

Alternatively, farnesylation of dansyl-GCVIA by PFTase was measured using an HPLC assay, similar to that of Pompliano et al. (1992a). A mixture (250 μL) of peptide, [^{3}H]FPP (250 mCi/mmol, 10 μM), and PFTase (1.5 nM) in 50 mM Tris HCl, 10 mM $MgCl_2$, 10 μM $ZnCl_2$, 5 mM DTT, 0.4% (w/v) Tween-80 or 0.04% (w/v) *n*-dodecyl-β-D-maltoside, pH 7.0, was incubated at 30 °C for 5 min before the reaction was stopped by the addition of EDTA. A portion (200 μL) was analyzed by reversed-phase HPLC on a Varian Sp-C8-IP-5 column (4 × 150 mm) at 1.0 mL/min using a gradient of 45% B to 100% B over 15 min; solvent A was 25 mM NH_4HCO_3, and solvent B was acetonitrile.

To examine the ability of PFTase to farnesylate short peptides, a TLC assay similar to one described by Goldstein et al. (1991) was used. Peptides were incubated with [^{3}H]-FPP (500 mCi/mmol, 20 μM) and 1.6 nM PFTase in 50 mM Tris HCl, 10 mM $MgCl_2$, 10 μM $ZnCl_2$, 5 mM DTT, 0.04% (w/v) *n*-dodecyl-β-D-maltoside, pH 7.0 (50 μL), for 10 min at 30 °C. The reactions were stopped by the addition of EDTA, and a 12 μL portion of the mixture was spotted onto 5 × 18 cm analytical aluminum-backed silica TLC plates (Whatman) and dried. The plates were eluted with *n*-propanol:water (7:3). The plates were dried and cut into 1.5 cm pieces. Scintillation fluid [CytoScinct (ICN), 10 mL] was added, and the samples were counted.

Measurement of the Dissociation Constant for FPP. To [^{3}H]FPP (3.3 Ci/mmol, 100−1000 nM) in 50 mM Tris HCl, 10 mM $MgCl_2$, 10 μM $ZnCl_2$, pH 7.0 (100 μL final volume) was added PFTase (3 μg). The mixtures were incubated at 30 °C for 20 min. A sample (10 μL) was removed from the tube and mixed with 10 mL of CytoScint (ICN) to determine the total radioactivity of the sample. The remainder of the mixture was transferred to the top sample compartment of a preequilibrated Microcon-30 concentrator (Amicon) and centrifuged at full speed (14 000 rpm) in a microcentrifuge for 8 s or until approximately 10−15 μL of the mixture had passed through the membrane. A 10 μL portion of the filtrate was removed to determine the concentration of free substrate. The radioactivity was corrected for membrane retention using a correction factor obtained from an identical experiment as described above except that enzyme was omitted.

Statistical Analysis. Initial reaction rates were determined using software provided with the Spex FluoroMax model spectrofluorimeter. Kinetic constants were determined by explicit or simple weighted nonlinear regression analysis utilizing Grafit (Erithicus Software, Staines, U.K.) or by a FORTRAN program employing the nonlinear least-squares optimizing routine STEPIT (Chandler, 1976). Standard errors for the fitted kinetic parameters correspond to the diagonal elements of the error matrix generated during the fitting routines (Bevington & Robinson, 1992).

RESULTS

Steady-State Kinetic Studies. Initial velocities for the alkylation of the cysteine in dansyl-GCVIA by FPP were measured by the continuous fluorescence assay of Pompliano et al. (1992b). This assay measures the increase in fluores-

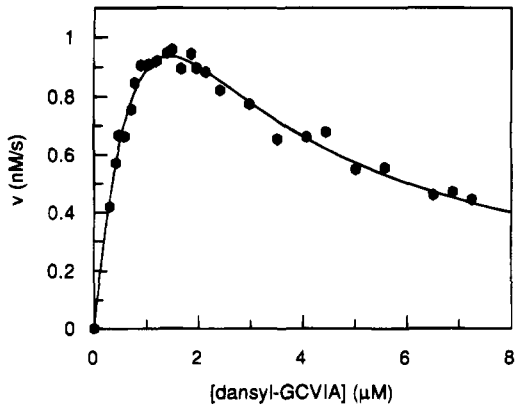

FIGURE 1: Substrate inhibition of PFTase by dansyl-GCVIA. Assays contained 5 μM FPP, dansyl-GCVIA (0.3−7.25 μM), and PFTase (0.64 nM).

cence of a dansylated pentapeptide upon farnesylation. We found it necessary to use *n*-dodecyl-β-D-maltoside (0.04% w/v) as the detergent in order to obtain a stable fluorescence signal (Cassidy et al., 1995). With dansyl-GCVIA, a more suitable substrate for yeast PFTase, exciting at 340 nm and monitoring the farnesylation at 486 nm produced a 10−15-fold enhancement of the fluorescence.

When the dansyl-GCVIA was varied at a fixed concentration of FPP (5 μM), the rate initially increased then decreased (Figure 1). The data were fitted to a standard form of the Michaelis−Menten equation modified for substrate inhibition

$$v = \frac{V_{Max}D}{K_M + D(1 + D/K_i)} \quad (1)$$

where D is the concentration of dansyl-GCVIA and K_i is the substrate inhibition constant (K_i = 1.1 μM). Substrate inhibition was also observed with dansyl-GCVLS and dansyl-GCVIM (data not shown). In order to confirm that the observed substrate inhibition was not an artifact of the fluorescence assay, the reaction between dansyl-GCVIA and [^{3}H]FPP was monitored using an HPLC assay (Pompliano et al., 1992a). Substrate inhibition was also observed with this assay. The dansyl moiety was not solely responsible for the inhibition, as neither dansylamide nor dansylglycine was an inhibitor up to a concentration of 200 μM.

The pattern for the variation of the slopes and intercepts from a double-reciprocal plot of initial velocities versus the concentration of FPP at a series of fixed concentrations of dansyl-GCVIA is typical of what one would expect for inhibition by the peptide substrate (Segel, 1975). Figure 2 displays replots of the intercepts and slopes from a double-recriprocal plot of initial velocities versus the concentration of FPP as a function of inverse peptide concentration. The linear behavior in Figure 2a indicates the apparent maximal reaction velocity for FPP as a function of peptide concentration D is not affected by the inhibition. By contrast, the replot of the slopes (Figure 2b) versus the reciprocal of the peptide concentration is affected by the inhibition, as indicated by the upward curvature. Since the dependence shown in Figure 2a is linear, the curvature in Figure 2b must result from a change in the apparent Michaelis constant for FPP. In fact, the K_Ms for FPP vary from 0.5 μM at 0.8 μM peptide up to 48 μM at 6.5 μM peptide, almost 2 orders of magnitude.

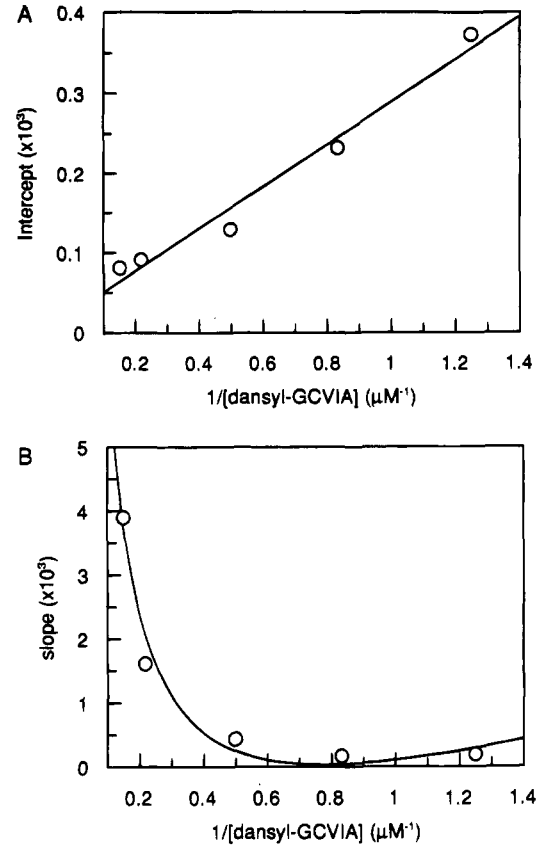

FIGURE 2: Secondary plots from a double-reciprocal plot of initial velocities versus the concentration of FPP at a series of fixed concentrations of dansyl-GCVIA. (A) Intercepts versus the reciprocal of dansyl-GCVIA concentration. (B) Slopes versus the reciprocal of dansyl-GCVIA concentration.

The Michaelis−Menten reaction rate equation for a mechanism that accounts for this behavior (Segel, 1975; Laskovics et al., 1979) is given by

$$v = \frac{V_{Max}DF}{(1 + D/K_I)(K_D K_M^D + K_M^F D) + K_M^D F + FD} \quad (2)$$

where F is the concentration of FPP, V_{Max} is the global maximum reaction velocity, K_I is the substrate inhibition constant associated with the ED* = E + D equilibrium, K_M^F and K_M^D are the Michaelis constants for FPP and dansyl-GCVIA at infinite second substrate concentrations, respectively, and K_D is the dissociation constant for the E·FPP complex. However, due to the number of kinetic parameters in eq 2, we were unable to obtain a satisfactory fit of the data.

Very high FPP concentrations (300 μM) can overcome the substrate inhibition even at high peptide concentration (15 μM) (data not shown). At these concentrations, the initial velocity rate equation simplifies to

$$v = \frac{V_{Max}D}{K_M^D + D} \quad (3)$$

where V_{Max} is the global maximal velocity and K_M^D is the Michaelis constant for the peptide. Initial velocity data fit to eq 3 gave V_{Max} = 3.4 ± 0.5 μmol min^{-1} mg^{-1} (k_{cat} = 4.5 ± 1 s^{-1}) and K_M^D = 1.7 ± 0.5 μM.

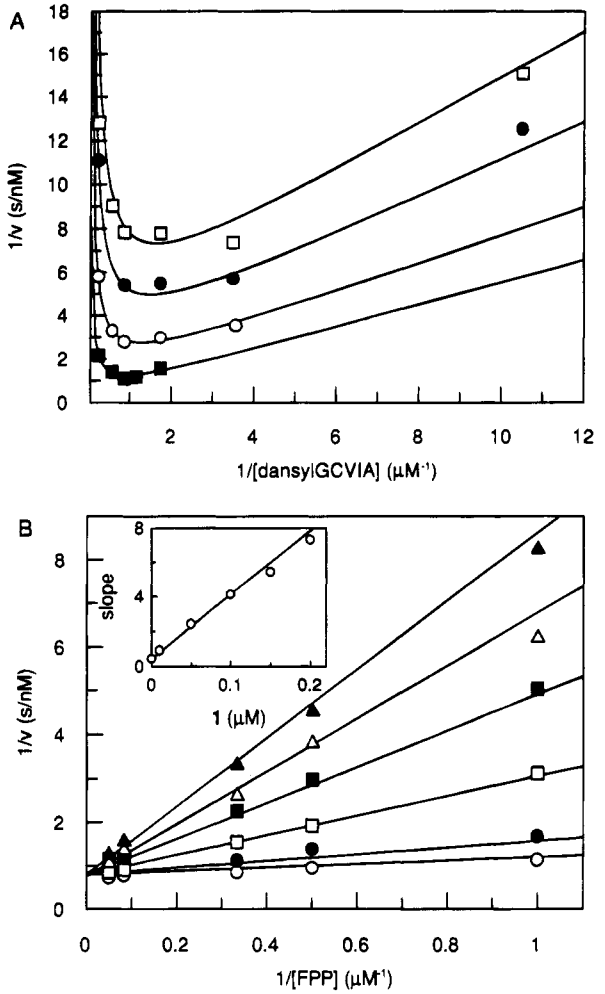

FIGURE 3: Inhibition of PFTase with 13-trifluoroFPP. (A) Double-reciprocal plot with dansyl-GCVIA as the varied substrate at fixed concentrations of 13-trifluoroFPP. Concentrations of 13-trifluoroFPP were 0 (○), 0.02 (●), 0.06 (□), 0.15 (■), and 0.25 (▲) μM. The concentration of FPP was 2.0 μM. (B) Double-reciprocal plot with FPP as the varied substrate at fixed concentrations of 13-trifluoroFPP. Concentrations of 13-trifluoroFPP were 0 (○), 0.01 (●), 0.05 (□), 0.1 (■), 0.15 (△), and 0.2 (▲) μM. The concentration of dansyl-GCVIA was 2.4 μM. Inset. Slopes versus the concentrations of 13-trifluoroFPP.

Kinetic Studies with Dead-End Inhibitors. 13-TrifluoroFPP, an analog of FPP containing a trifluoromethyl group

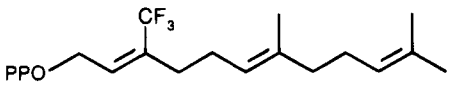

13- trifluorofarnesyl diphosphate

at C3, was recently synthesized for a linear free energy study of PFTase (Dolence & Poulter, 1995) and was found to be 770-fold less reactive than FPP itself. Thus, for practical purposes, 13-trifluoroFPP is a dead-end inhibitor of the PFTase reaction with normal substrates. Double-reciprocal plots of initial velocities for varied FPP and dansyl-GCVIA at different fixed concentrations of 13-trifluoroFPP are shown in Figure 3. When dansyl-GCVIA was the varied substrate, the plots showed a dramatic upward curvature at high peptide concentrations characteristic of substrate inhibition, while linear plots were obtained for varied FPP. The best fits were obtained when 13-trifluoroFPP was treated as a noncompetitive inhibitor for varied peptide and a competitive inhibitor for varied FPP. The curves shown in Figure 3 were calculated from fits of the kinetic data to the appropriate forms of the Michaelis–Menten equation, and the results are summarized in Table 1.

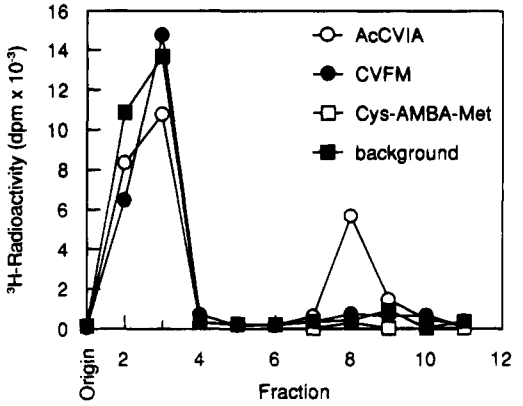

FIGURE 4: Determination of non-farnesylated peptides by thin-layer chromatography. TLC assays were performed as described in the Materials and Methods section.

In order to identify nonsubstrate peptide inhibitors for yeast PFTase, candidates were incubated with [^{3}H]FPP and the reaction mixture was resolved by thin-layer chromatography after quenching. As shown in Figure 4, the known PFTase substrate Ac-ACVIA gave a product peak at the expected position (Goldstein et al., 1991), while no product was observed with the nonsubstrate SVIA (data not shown). Two unreactive peptide analogs were found. The tetrapeptide CVFM had an IC_{50} = 0.4 μM, and the peptidomimetic Cys-AMBA-Met (Nigam et al., 1993) was less potent (IC_{50} = 5.0 μM). In addition, ACV(D)IA, containing a D-isoleucine in the CaaX sequence, was not farnesylated (data not shown) but was a poor inhibitor of PFTase (IC_{50} = 435 μM).

The results with Cys-AMBA-Met as an inhibitor against both FPP and dansyl-GCVIA are summarized in Table 1, and double-reciprocal plots are shown in Figure 5. Cys-AMBA-Met was competitive against dansyl-GCVIA and uncompetitive against FPP. Although CVFM was a good dead-end inhibitor (IC_{50} = 0.4 μM), attempts to use CVFM gave poor fits. The steady-state inhibition patterns for 13-trifluoroFPP and Cys-AMBA-Met are consistent with an ordered sequential mechanism (Segel, 1975).

Results from product inhibition studies also support an ordered mechanism. Inorganic diphosphate (PP_i) was noncompetitive against both FPP and dansyl-GCVIA (Table 1). However, farnesylated peptides did not inhibit yeast PFTase. Table 2 shows the farnesylated cysteines and peptides that were screened as potential product inhibitors. Of these, only KTSC^{F}VFM displayed a significant level of inhibition. Unfortunately, this activity was observed only at high detergent concentrations (0.4% Tween-80) incompatible with the fluorescence assay. The IC_{50} value listed was determined using the HPLC assay.

FPP Dissociation Constant. A membrane filter assay was used to determine the dissociation constant for the E·FPP complex (Song and Poulter, private communication). [^{3}H]-FPP was sufficiently hydrophobic that some of the radiolabeled substrate was retained by the membrane. From control reactions carried out with buffer in place of PFTase, a retention factor for FPP of 1.6 was calculated. Attempts to

Table 1: Inhibition Patterns and Constants of Dead-End and Product Inhibitors of PFTase

	with respect to FPP		with respect to dansyl-GCVIA	
compd	pattern	K_i (μM)	pattern	K_i (μM)
13-trifluoroFPP	competitive	$K_i = 0.011 \pm 0.002$	noncompetitive	$K_{is} = 0.29 \pm 0.05$ $K_{ii} = 0.022 \pm 0.004$
Cys-AMBA-Met	uncompetitive	$K_i = 2.0 \pm 0.1$	competitive	$K_i = 0.79 \pm 0.07$
PP_i	noncompetitive	$K_{is} = 2400 \pm 200$ $K_{ii} = 1200 \pm 200$	noncompetitive	$K_{is} = 3000 \pm 130$ $K_{ii} = 1300 \pm 50$

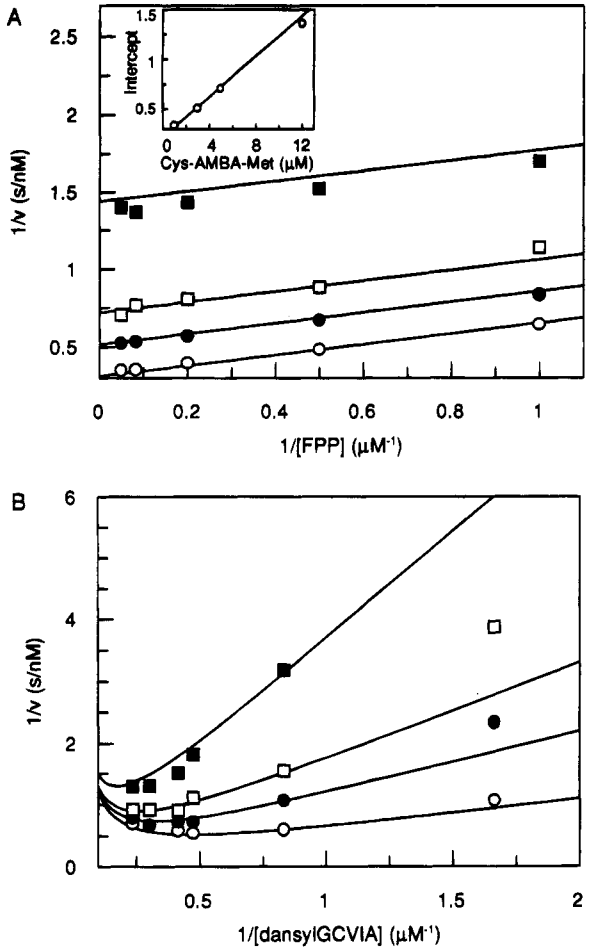

FIGURE 5: Inhibition of PFTase with Cys-AMBA-Met. (A) Double-reciprocal plot with FPP as the varied substrate at fixed concentrations of Cys-AMBA-Met. Concentrations of Cys-AMBA-Met were 1 (○), 3 (●), 5 (□), and 12 (■) μM. The concentration of dansyl-GCVIA was 2.4 μM. Inset. Intercepts versus the concentrations of Cys-AMBA-Met. (B) Double-reciprocal plot with dansyl-GCVIA as the varied substrate at fixed concentrations of Cys-AMBA-Met. Concentrations of inhibitor were 1 (○), 3 (●), 5 (□), and 12 (■) μM. The concentration of FPP was 2.0 μM.

diminish the retention of FPP by adding *n*-dodecyl-β-D-maltoside to the assay buffer increased the factor to 2.5.

After correcting for membrane retention, the measured value for free [^{3}H]FPP concentration was subtracted from the total FPP concentration to obtain the concentration of enzyme-bound [^{3}H]FPP. The data were then fitted to a standard binding equation (Fersht, 1985) to obtain K_D and the number of binding sites per mole of enzyme. With 225 nM PFTase, duplicate measurements at six [^{3}H]FPP concentrations yielded $K_D = 75 \pm 15$ nM and a capacity of 380 $\pm$ 20 nM, or 1.7 binding sites per mole of enzyme (data not shown). The number of binding sites is higher than the expected value of unity and might arise from uncertainties

Table 2: Farnesylated Amino Acids and Peptides Examined as Product Inhibitors of PFTase

compound	IC_{50} (μM)
S-farnesylcysteine	>250
S-farnsylcysteine methyl ester	>200
N-acetyl-*S*-farnesylcysteine methyl ester	>150
C^FVIA	>200
N-acetyl-C^FVIA	>150
AC^FVLS	200[a]
$KTSC^FVIA$	70[b]

[a] 25% inhibition observed using the HPLC assay (see Materials and Methods). [b] IC_{50} value determined using the HPLC assay (see Materials and Methods).

Table 3: Summary of Progress Curve Fits[a]

run no.	[D][b]	[D] (fit)[c]	K_M^D	k_{cat} (s^{-1})
1	0.5	0.73	0.77	6.19
2	0.5	0.70	0.67	2.43
3	1.0	1.14	0.91	6.02
4	1.0	0.86	1.05	2.41
5	1.0	0.80	0.81	2.99
6	3.0	2.85	0.98	6.78
av			0.9 ± 0.1	4.5 ± 1.9

[a] [FPP] = 100 μM for all measurements. PFTase (0.5−1.5 nM) was used to initiate the reactions. Each run (1−6) represents the average of duplicate determinations. Progress curves were followed for 15−30 min. Peptide concentrations and Michaelis constants have units of μM. [b] Starting peptide concentration. [c] Peptide concentration after fit.

in the enzyme concentration as determined by the Bradford assay.

Progress Curves. Because of difficulties in obtaining an accurate value for V_{Max} in a system showing severe substrate inhibition, we measured progress curves for 0.5−3 μM dansyl-GCVIA and 100 μM FPP using the fluorescence assay. The data were fitted to the integrated form of eq 3, eq 4 (below)

$$t = \frac{1}{V_{Max}}\left[P(t) + K_M{}^D \ln\left(\frac{D_0}{D_0 - P(t)}\right)\right] \quad (4)$$

where D_0 is the starting dansyl-GCVIA concentration and $P(t)$ is the time-dependent product concentration (Orsi & Tipton, 1979; Laskovics et al., 1979). Both the reactant D and product P emit at 486 nm, so the observed fluorescence F_{obs} must be corrected in order to obtain only the product fluorescence. This was accomplished according to eq 5:

$$P(t) = [e/(e - 1)](1/m)[F_{obs}(t) - F_{obs}(t=0)] \quad (5)$$

where e is the fluorescence enhancement factor (e = 10−11) and m ($m = 3.8 \times 10^6$ cps/μM) is the conversion factor (see Materials and Methods). Progress curves were composed of 90−180 individual data points. Due to the large

Scheme 2. Scheme for an Ordered Bireactant Mechanism with Substrate Inhibition

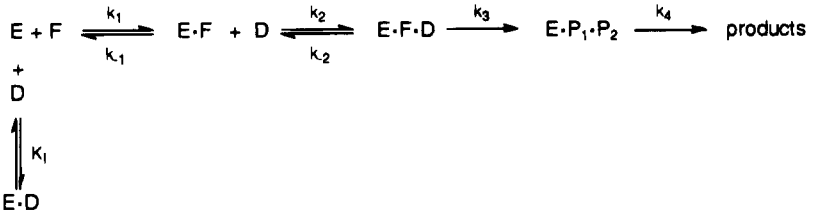

number of points, the fitted curves were superimposible with the measured curves (data not shown).

The results for six progress curves are listed in Table 3. Since small dilution errors as well as minor variations in the conversion factor m can significantly affect the measured product fluorescence, the starting concentration of peptide must be treated as an independent parameter (Orsi & Tipton, 1979). The second column in Table 3 shows the starting peptide concentrations in the assay, while the third column shows the apparent peptide concentration that minimizes χ^2. The differences between the second and third columns are not large. The fourth and fifth columns list values for K_M^D and k_{cat} obtained for each progress curve, respectively. Averaging the six values for each constant gave $K_M^D = 0.9 \pm 0.1$ μM and $k_{cat} = 4.5 \pm 1.9$ s^{-1}.

DISCUSSION

In contrast to previous studies with PFTase from mammalian sources, kinetic studies with yeast PFTase and dead-end substrate inhibitors clearly support an ordered sequential mechanism with FPP binding first. 13-TrifluoroFPP, a competitive inhibitor with respect to FPP, displays a non-competitive pattern when the peptide is the varied substrate. Cys-AMBA-Met is a competitive inhibitor with respect to the peptide but is an uncompetitive inhibitor with respect to FPP. Product inhibition studies with PP_i showed noncompetitive inhibition patterns with both substrates, also in support of an ordered mechanism. Interestingly, farnesylated peptides did not inhibit PFTase. While the insolubility of these products under our assay conditions may explain the lack of inhibition, others have observed product inhibition with farnesylated peptides of PFTase from bovine brain in the low micromolar range (Pompliano et al., 1992a).

A minimal kinetic mechanism consistent with the observations summarized in Figures 1 and 2 and the binding order studies (Figures 3 and 5) is shown in Scheme 2, in which E·D is a nonproductive complex. The patterns shown in Figure 2, a linear intercept vs 1/[FPP] and a curved slope vs 1/[FPP], are exactly those expected for substrate inhibition in an ordered sequential mechanism in which nonproductive binding of the second substrate is competitive with binding of the first (Segel, 1975). In an ordered sequential mechanism, substrate inhibition is often due to interception of an enzyme product complex by substrate (Segel, 1975; Hupe et al., 1986; Cleland, 1979). However, this type of inhibition gives curved intercept and linear slope replots. In addition, the substrate inhibition cannot be overcome at high levels of the other substrate.

Although we are the first to fully characterize substrate inhibition in a protein prenyltransferase, several other examples have been reported. In early studies with rat PFTase, a decrease in rate with increasing peptide concentrations was observed using N-acetylated tetrapeptides (Brown et al., 1992). At high concentrations of Ras-CVIM, substrate inhibition was also noted in studies with human PFTase (Pompliano et al., 1993). In addition, substrate inhibition does not appear to be limited to the farnesyltransferases. Yokoyama et al. (1995) observed inhibition of PGGTase I with biotinylated peptide substrates. The enhanced sensitivity of yeast PFTase relative to its mammalian counterparts is probably due to differences in the relative affinities of the enzymes for their diphosphate and peptide substrates. Yeast PFTase has a somewhat lower affinity for peptide than the mammalian enzymes. For example, the yeast enzyme could not be purified by affinity chromatography on peptide-linked supports using procedures that were highly successful for mammalian PFTases (Mayer et al., 1993), and the K_Ms for peptide substrates are higher for yeast by a factor of 3−4. However, the affinity for FPP, as measured by K_D, is also lower; up to 35-fold for yeast PFTase relative to the mammalian enzymes. Since an increase in the concentration of FPP requires a corresponding increase in the concentration of peptide needed to detect substrate inhibition for yeast PFTase, the onset may not be seen for mammalian enzymes at substrate concentrations used for kinetic measurements. In any case, substrate inhibition should not be manifest under normal physiological conditions where anticipated levels of peptide and FPP range between low nanomolar and low micromolar concentrations (Bruenger & Rilling, 1988; Pompliano et al., 1993). Furthermore, the very tight binding seen for FPP ensures that a sufficient level of the substrate will always be available for prenylation of proteins *in vivo*, even as the concentration of FPP fluctuates as a consequence of regulation of sterol biosynthesis.

Our results show that peptides bind to free yeast PFTase in a manner that precludes the productive binding of FPP. A related case of substrate inhibition has been reported for another prenyltransferase (Laskovics et al., 1979). Farnesyl diphosphate synthase (FPPSase) catalyzes the elongation of isoprenoid chains by a prenyl transfer reaction. In this case, the substrate that accepts the isoprenoid moiety, isopentenyl diphosphate (IPP), closely resembles the allylic substrate dimethylallyl diphosphate (DMAPP), and it is easy to rationalize the inhibition of FPPSase by IPP. It is less clear why a peptide or protein should bind to the corresponding allylic site in PFTase. Perhaps the hydrophobic side chains in the peptide interact with the region of the catalytic site that normally binds the farnesyl moiety. Alternatively, the peptide might sterically block entry of FPP or prevent a conformational change required for FPP binding. Furfine et al. (1995) reported evidence for a conformational change upon binding of FPP in the absence peptide using stopped-flow fluorescence measurements. They concluded FPP binds to PFTase in a two-step process that involves a conformational change in the enzyme−substrate complex in the second step. Productive binding of peptide then follows.

Scheme 3. Ordered Bireactant System with Substrate Inhibition and Dead-End Inhibitors

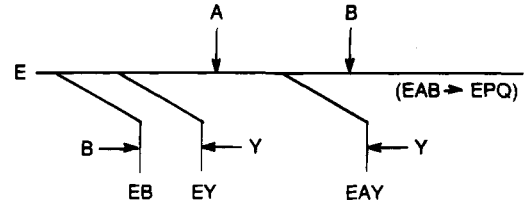

Because of the high degree of homology in the amino acid sequences of PFTases from different sources (Armstrong et al., 1993), one might expect that the mechanism for binding substrates would be similar. Initially, a random mechanism was proposed on the basis of inhibition studies with the enzyme from bovine brain (Pompliano et al., 1992a). For the reaction catalyzed by the human PFTase, similar experiments also supported a random mechanism (Pompliano et al., 1993). However, isotope-partioning studies showed that 80% of the FPP in a human PFTase–[^{3}H]FPP binary complex was trapped as the farnesylated product by saturating concentrations of Ras protein (Pompliano et al., 1993). In a similar study by Furfine et al. (1995), all of the FPP in an FPP–enzyme complex was converted to product. Thus, binding of FPP to free enzyme is not an equilibrium process in the presence of the prenyl acceptor, and FPP is a very "sticky" substrate with a high commitment to catalysis (Rose, 1980). In contrast, preformed PFTase–peptide or PFTase–Ras binary complexes were not trapped by added FPP (Furfine et al., 1995; Pompliano et al., 1993). These results are consistent with the ordered addition of FPP and peptide we found for the yeast enzyme. In addition, Yokoyama and Gelb (1995) were unable to trap the binary complex PGGTase I–biotin-γ-6-(L) with [^{3}H]GGPP, indicating that the farnesyl and geranylgeranyltransferases have similar mechanisms.

The difficulties one encounters in distinguishing between random and ordered mechanisms by steady-state kinetic measurements with an enzyme that shows substrate inhibition have been discussed for FPPSase (Laskovics et al., 1979). In this case, kinetic studies, including an analysis of Lineweaver–Burk plots for both product and dead-end inhibitors, suggested that the binding order was random, while isotope trapping experiments clearly demonstrated an ordered process. The reason for this apparent inconsistency becomes clear upon examination of the binding mechanism for FPPSase (see Scheme 3), where the allylic substrate (A) binds before IPP (B). In this case, where the structures of A and B were similar, B bound to the A site to form an inactive EB complex as well as to the B site in EA. In a similar manner, Y, an unreactive analog of B, bound to both E and EA. The resulting Lineweaver–Burk plots for inhibition by Y were typical of those expected for a random mechanism. In particular, the affinity of Y for the A site introduced an inhibitor-dependent term into the equation for v^{-1} versus [A] at different fixed concentrations of Y. This transforms the uncompetitive profile expected for a dead-end inhibitor in an ordered mechanism into a noncompetitive pattern typical of a random addition of A and B. A similar scenario might explain why the mammalian enzymes give profiles characteristic of a random mechanism while isotope-trapping demands an ordered process.

Whether an uncompetitive or noncompetitive Lineweaver–Burk plot is seen depends on the magnitude of the inhibition constant for addition of Y to E. Thus, enzymes can have similar binding mechanisms but give different double-reciprocal plots depending on the range of concentrations of substrates and inhibitors used in the kinetic measurements and the relative values of intrinsic rate constants. The combined results of steady-state and nonsteady-state kinetic studies indicate that PFTases bind FPP and peptide in an ordered manner.

ACKNOWLEDGMENT

We thank Dr. Andrew D. Hamilton for the generous gift of Cys-AMBA-Met.

REFERENCES

Armstrong, S. A., Seabra, M. C., Sudhof, T. C., Goldstein, J. L., & Brown, M. S. (1993) *J. Biol. Chem. 268*, 12221–12229.

Bevington, P. R., & Robinson, D. K. (1992) *Data Reduction and Error Analysis for the Physical Sciences*, 2nd ed., pp 141–167, McGraw-Hill, Inc., New York.

Bradford, M. M. (1976) *Anal. Biochem. 72*, 248–254.

Brown, M. J., Milano, P. D., Lever, D. C., Epstein, W. M., & Poulter, C. D. (1991) *J. Am. Chem. Soc. 113*, 3176–3177.

Brown, M. S., Goldstein, J. L., Paris, K. J., Burnier, J. B., & Marsters, J. C., Jr. (1992) *Proc. Natl. Acad. Sci. U.S.A. 89*, 8313–8316.

Bruenger, E., & Rilling, H. C. (1988) *Anal. Biochem. 173*, 321–327.

Cassidy, P. B., Dolence, J. M., & Poulter, C. D. (1995) *Methods Enzymol. 250*, 30–43.

Chandler, J. P. (1976) *Q.C.P.E. 11*, 307.

Clarke, S. (1992) *Annu. Rev. Biochem. 61*, 355–386.

Cleland, W. W. (1979) *Methods Enzymol. 63*, 500–513.

Davisson, V. J., Woodside, A. B., Neal, T. R., Stremler, K. E., Muehlbacher, M., & Poulter, C. D. (1986) *J. Org. Chem. 51*, 4768–4779.

Dolence, J. M., & Poulter, C. D. (1995) *Proc. Natl. Acad. Sci. U.S.A. 92*, 5008–5011.

Farnsworth, C. C., Kawata, M., Yoshida, Y., Takai, Y., Gelb, M. H., & Glomset, J. A. (1991) *Proc. Natl. Acad. Sci. U.S.A. 88*, 6196–6200.

Fersht, A. (1985) *Enzyme Structure and Mechanism*, Chapter 6, W. H. Freeman and Co., New York.

Furfine, E. S., Leban, J. J., Landavazo, A., Moomaw, J. F., & Casey, P. J. (1995) *Biochemistry 34*, 6857–6862.

Gibbs, J. B., Pompliano, D. L., Mosser, S. D., Rands, E., Lingham, R. B., Singh, S. B., Scolnick, E. M., Kohl, N. E., & Oliff, A. (1993) *J. Biol. Chem. 268*, 7617–7620.

Goldstein, J. L., Brown, M. S., Stradley, S. J., Reiss, Y., & Gierasch, L. M. (1991) *J. Biol. Chem. 266*, 15575–15578.

Gomez, R., Goodman, L. E., Tripathy, S. K., O'Rourke, E., Manne, V., & Tamanoi, F. (1993) *Biochem. J. 289*, 25–31.

Hupe, D. J., Azzolina, B. A., & Behrens, N. D. (1986) *J. Biol. Chem. 261*, 8363–8369.

James, G. L., Goldstein, J. L., Brown, M. S., Rawson, T. E., Somers, T. C., McDowell, R. S., Crowley, C. W., Lucas, B. K., Levinson, A. D., & Marsters, J. C., Jr. (1993) *Science 260*, 1937–1942.

Kohl, N. E., Mosser, S. D., deSolms, S. J., Giuliani, E. A., Pompliano, D. L., Graham, S. L., Smith, R. L., Scolnick, E. M., Oliff, A., & Gibbs, J. B. (1993) *Science 260*, 1934–1937.

Laskovics, F. M., Krafcik, J. M., & Poulter, C. D. (1979) *J. Biol. Chem. 254*, 9458–9463.

Marsters, J. C., Jr., McDowell, R. S., Reynolds, M. E., Oare, D. A., Somers, T. C., Stanley, M. S., Rawson, T. E., Struble, M. E., Burdick, D. J., Chan, K. S., Duarte, C. M., Paris, K. J., Tom, J. Y. K., Wan, D. T., Xue Y., & Burnier J. P. (1994) *Bioorg. Med. Chem. Lett. 2*, 949–957.

Mayer, M. P., Prestwich, G. D., Dolence, J. M., Bond, P. D., Wu, H.-Y., & Poulter, C. D. (1993) *Gene 132*, 41–47.

Moores, S. L., Schaber, M. D., Mosser, S. D., Rands, E., O'Hara, M. B., Garsky, V. M., Marshall, M. S., Pompliano, D. L., & Gibbs, J. B. (1991) *J. Biol. Chem. 266*, 14603−14610.

Nigam, M., Seong, C.-M., Hamilton, A. D., & Sebti, S. M. (1993) *J. Biol. Chem. 268*, 20695−20698.

Omer, C. A., Krai, A. M., Diehl, R. E., Prendergast, G. C., Powers, S., Allen, C. M., Gibbs, J. B., & Kohl, N. E. (1993) *Biochemistry 32*, 5167−5176.

Orsi, B. A., & Tipton, K. F. (1979) *Methods Enzymol. 63*, 159−183.

Pompliano, D. L., Rands, E., Schaber, M. D., Mosser, S. D., Anthony, N. J., & Gibbs, J. B. (1992a) *Biochemistry 31*, 3800−3807.

Pompliano, D. L., Gomez, R. P., & Anthony, N. J. (1992b) *J. Am. Chem. Soc. 114*, 7945−7946.

Pompliano, D. L., Schaber, S. D., Omer, C. A., Shafer, J. A., & Gibbs, J. B. (1993) *Biochemistry 32*, 8341−8347.

Reiss, Y., Stradley, S. J., Gierasch, L. M., Brown, M. S., & Goldstein, J. L. (1991) *Proc. Natl. Acad. Sci. U.S.A. 88*, 732−736.

Rose, I. A. (1980) *Methods Enzymol. 64*, 47−59.

Schafer, W. R., Kim, R., Stern, R., Thorner, J., Kim, S.-H., & Rine, J. (1989) *Science 245*, 379−385.

Segel, I. H. (1975) *Enzyme Kinetics*, Chapters 5 and 9, John Wiley, New York.

Tamanoi, F. (1993) *Trends Biochem. Sci. 18*, 349−353.

Vogt, A., Qian, Y., Blaskovich, M. A., Fossum, R. D., Hamilton, A. D., & Sebti, S. M. (1995) *J. Biol. Chem. 270*, 660−664.

Wai, J. S., Bamberger, D. L., Fisher, T. E., Graham, S. L., Smith, R. L., Gibbs, J. B., Mosser, S. D., Oliff, A. I., Pompliano, D. L., Rands, E., & Kohl, N. E. (1994) *Bioorg. Med. Chem. Lett. 2*, 939−947.

Yokoyama, K., Goodwin, G. W., Ghomashchi, F., Glomset, J. A., & Gelb, M. H. (1991) *Proc. Natl. Acad. Sci. U.S.A. 88*, 5302−5306.

Yokoyama, K., McGeady, P., & Gelb, M. H. (1995) *Biochemistry 34*, 1334−1354.

Zhang, F. L., Diehl, R. E., Kohl, N. E., Gibbs, J. B., Giros, B., Casey, P. J., & Omer, C. A. (1994) *J. Biol. Chem. 269*, 3175−3180.

BI951939D